Preprint Title	Green SPIONs as a novel highly selective treatment for leishmaniasis: an *in vitro* study against *Leishmania amazonensis* intracellular amastigotes
Authors	Brunno R. F. Verçoza, Robson R. Bernardo, Luiz Agusto S. de Oliveira and Juliany C. F. Rodrigues
Publication Date	24 Apr. 2023
Article Type	Full Research Paper
ORCID® iDs	Brunno R. F. Verçoza - https://orcid.org/0000-0001-6117-7879; Luiz Agusto S. de Oliveira - https://orcid.org/0000-0002-4034-8365; Juliany C. F. Rodrigues - https://orcid.org/0000-0001-6807-8101

Green SPIONs as a novel highly selective treatment for leishmaniasis: an *in vitro* study against *Leishmania amazonensis* intracellular amastigotes

Brunno R. F. Verçoza[1], Robson R. Bernardo[1,2], Luiz Augusto S. de Oliveira[1,2] and

Juliany C. F. Rodrigues[1*]

[1] Núcleo Multidisciplinar de Pesquisas em Biologia, NUMPEX-Bio, Campus UFRJ Duque de Caxias Prof. Geraldo Cidade, Universidade Federal do Rio de Janeiro, Rodovia Washington Luiz, n. 19593, km 104.5, 25240-005, Duque de Caxias, RJ, Brasil

[2] Núcleo Multidisciplinar de Pesquisas em Nanotecnologia, NUMPEX-Nano, Campus UFRJ Duque de Caxias Prof. Geraldo Cidade, Universidade Federal do Rio de Janeiro, Rodovia Washington Luiz, n. 19593, km 104.5, 25240-005, Duque de Caxias, RJ, Brasil

* Correspondence Author:

Juliany Cola Fernandes Rodrigues

Email address: juliany.rodrigues@caxias.ufrj.br

Abstract

Objective: The main goal of this work was to evaluate the therapeutic potential of green SPIONs produced with coconut water for treating cutaneous leishmaniasis caused by *Leishmania amazonensis*. **Materials and methods:** Optical and electron microscopy techniques were used to evaluate the effects on cell proliferation, infectivity percentage,

and ultrastructure. **Results:** SPIONs were internalized by both parasite stages, randomly distributed by the cytosol located mainly in membrane-bound compartments. The selectivity index for intracellular amastigotes was higher than 240 times compared to current drugs used to treat the disease. **Conclusion:** The synthesized SPIONs showed an important and promising anti-*Leishmania* activity and can be considered a strong candidate for a new therapeutic approach for treating leishmaniases.

Introduction

Leishmaniasis is one of the most important neglected diseases of chronic nature that remains a serious global health problem. A worrying increase has been observed in the number of leishmaniasis cases worldwide in recent decades. It is estimated that about 600 million people are in risk areas, and 0.6 - 1.2 million new leishmaniasis cases appear annually [1]. The treatment for this disease involves using pentavalent antimonials, miltefosine, amphotericin B, paromomycin, or pentamidine. However, the side effects of these drugs and the increased number of drug-resistant parasites have been reported [2-5]. These facts demonstrate the need to develop new treatments or alternatives that are safer, more effective, and more accessible to patients.

In this context, Nanomedicine is being presented as one of the most promising branches of contemporary Medicine, currently concentrating a large part of the scientific efforts searching for new treatments for different diseases. Its main objective is to develop therapies with higher specificity, effectiveness, safety, and less toxicity

[6]. One interesting class of nanomaterials for the health sciences is the superparamagnetic iron oxide nanoparticles (SPIONs). SPIONs present theranostic properties and can be used simultaneously for diagnosis and therapy. Thus, the SPIONs have emerged as one of the best options for the development of new therapeutic alternatives with several features such as good biocompatibility, degradability in moderate acid conditions, magnetic manipulation, the possibility of being used in magnetic resonance image (MRI), and its ability to generate controlled heat non-invasively when subjected to an alternating current magnetic field (AMF) [7,8].

The application of SPIONs in treating leishmaniasis has been studied by different groups over the past few years, showing promise and satisfactory results [9-12]; thus, the use of SPIONs to develop new topical treatments can mean a revolution. Therefore, SPIONs should be used for topical application, whether associated with drugs and combined or not with thermotherapy by magnetic hyperthermia. Furthermore, this technology will allow the treatment to be applied to the localized cutaneous lesion, making the treatment more specific and less toxic to the patient.

Thus, the main goal of this study is to evaluate the effects of green SPIONs in *Leishmania amazonensis in vitro*.

Results

Uptake of SPIONs by *L. amazonensis* promastigotes and intracellular amastigotes using different microscopy techniques

Bright-field optical microscopy of the *L. amazonensis* promastigotes and intracellular amastigotes incubated with Prussian blue revealed that both parasite stages can uptake the SPIONs (Figures 1A-D). In these figures (arrows and arrowheads), it was possible to observe the presence of the characteristic blue stain, which indicates the

positive reaction between potassium ferrocyanide and ferrous compounds. In promastigotes (Fig. 1A-B), the SPIONS are distributed throughout the cytosol, as suggested by the images. On the other hand, in the intracellular amastigotes cultivated in macrophages, the SPIONs appeared in the mammalian cytosol, inside the parasitophorous vacuole, and in the parasite cytosol (Figs. 1C-D; arrows and arrowheads).
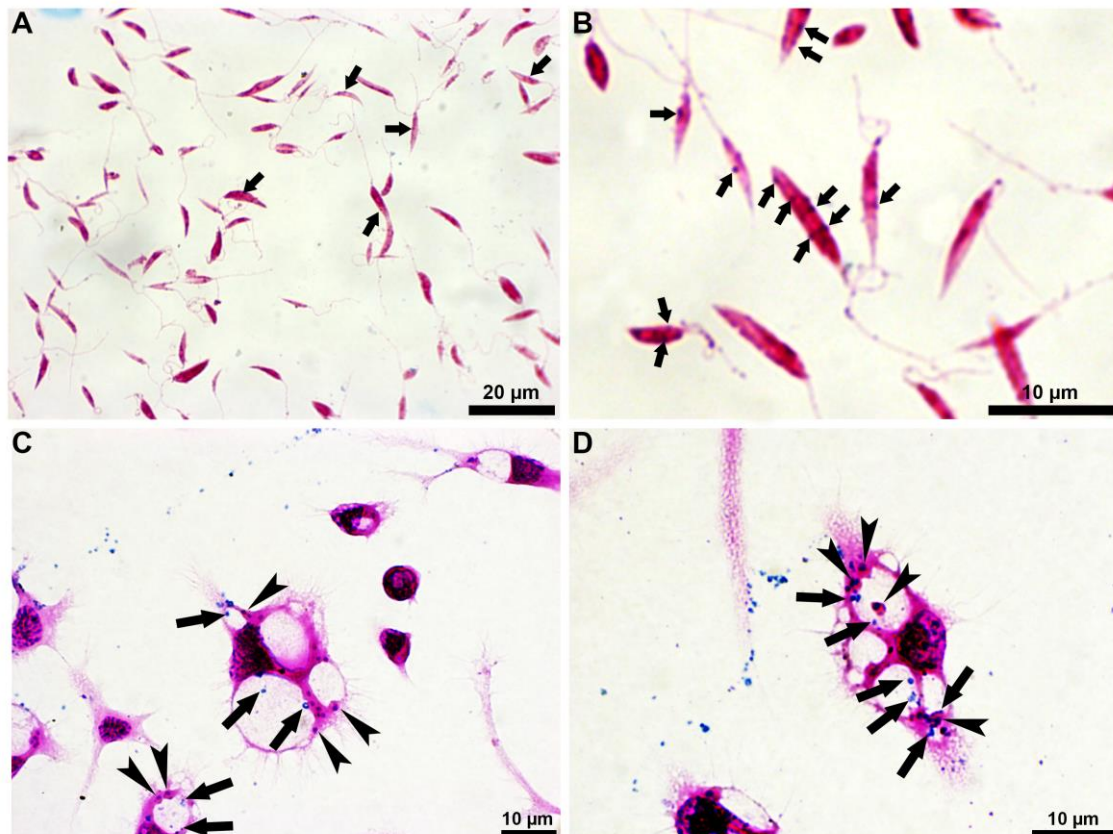
Figures 1A-D. Bright-field optical microscopy of *L. amazonensis* promastigotes **(A-B)** and intracellular amastigotes **(C-D)** treated with 100 µg/mL of SPIONS for 24 h after staining with Prussian blue **(A-D)**. **(A)** The arrows indicate the presence of the characteristic Prussian blue marking for the reaction with ferrous compounds in the promastigote cytosol. **(B)** Digital magnification shows that SPIONs are randomly distributed throughout the cytosol. **(C)** In the case of macrophages infected with intracellular amastigotes, the SPIONs were observed inside the parasitophorous vacuoles. **(D)** Digital magnification better shows the SPIONs (arrows) inside the macrophage cytosol, the parasitophorous vacuoles, and the amastigote cytosol (arrowheads).

After the first microscopic analysis, scanning electron microscopy (SEM) and chemical element mapping analysis were carried out to confirm the uptake of the SPIONs by *L. amazonensis* intracellular amastigotes after removing the plasma membrane to exposing the cytoplasmic environment (Figure 2A-D). Image from secondary electrons (SE) revealed the presence of intracellular amastigotes inside de parasitophorous vacuoles (Figure 2A). On the other hand, backscattered electron (BSE) showed the presence of several small electron-lucent structures randomly distributed throughout the macrophage cytosol, inside the parasitophorous vacuoles (Figure 2B, arrows) and the intracellular amastigotes (Figure 2B, arrowheads). Finally, the ferrous nature of observed structures was assessed by chemical element mapping analysis using X-ray spectroscopy by dispersive energy (Figure 2C), confirming that the electron-lucent structures are composed of iron atoms (Figure 2D).

Moreover, transmission electron microscopy (TEM) was used to confirm the internalization of the SPIONs. Firstly, promastigotes were treated with 100 µg/mL of SPIONs for 24 h (Fig. 3A-C). TEM images confirmed the presence of SPIONs aggregates randomly distributed throughout the cytoplasm of the promastigotes (Fig. 3A-C, arrowheads); the images suggest that these aggregates have different sizes. Furthermore, in high magnification, it is possible to observe that the SPIONS are frequently surrounded by membranes (Fig. 3B, arrow). In addition, the SPIONs were also observed inside the flagellar pocket (Fig. 3C, arrowheads) and closely associated with the membrane.
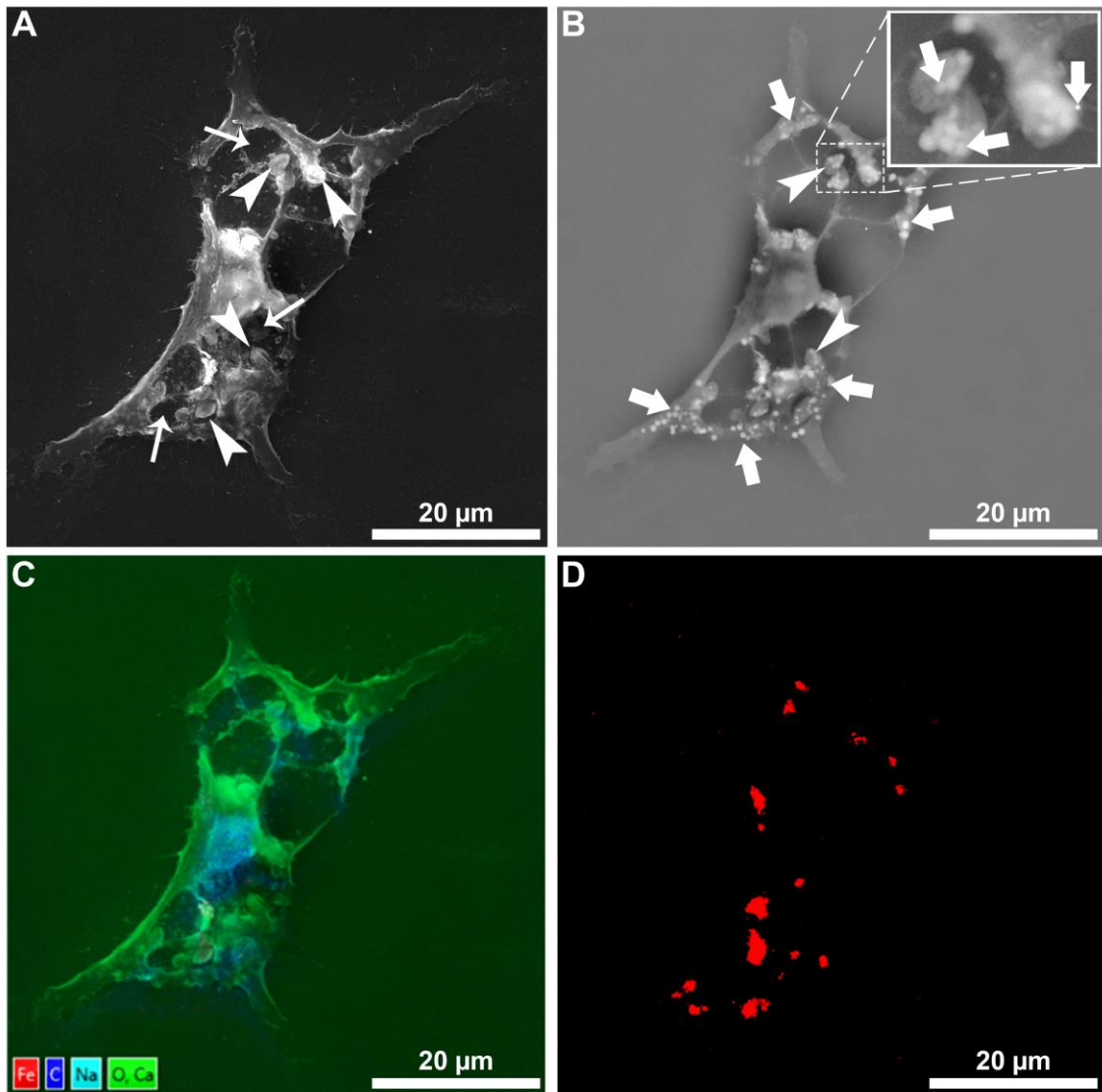
Figures 2A-D. Scanning electron microscopy of macrophages infected with *L. amazonensis* intracellular amastigotes after treatment with 100 µg/mL SPIONs for 24 h. The plasma membrane was gently removed to observe the presence of nanoparticles inside the cells. Panel **A** shows infected macrophages, where it is possible to observe some amastigotes (arrowheads) inside the parasitophorous vacuoles (thin arrow). Panel **B** shows the same macrophage; however, the image was obtained by detecting backscattered electrons, revealing several electron-lucent aggregates (arrows). Through digital magnification (highlight), it was possible to observe the presence of electron-lucent aggregates even inside intracellular amastigotes (arrowheads). Finally, panels **C** and **D** show the X-ray microanalysis mapping of infected macrophages, indicating the presence of iron in the cytosol (red color in figure 2D).

The uptake of SPIONs was also observed in macrophages infected with *L. amazonensis* intracellular amastigotes after treatment with 100 µg/mL of SPIONs for 24 h (Figs. 3D-F). The images confirmed the presence of the SPIONs aggregates inside the macrophage cytosol, the parasitophorous vacuoles, and the intracellular amastigotes (Figs. 3C-D, arrowhead). SPIONs were also observed inside the macrophages close to the parasitophorous vacuole membrane (Fig. 3D, large arrow), sometimes appearing inside membrane-bound structures and presenting different sizes (Fig. 3E, arrowhead). In this figure, some alterations in amastigote ultrastructure can also be observed as the presence of electron-lucent lipid bodies, a multivesicular body close to the Golgi complex, and endoplasmic reticulum profiles very close to organelles such as mitochondrion and glycosome. High magnification image revealed that the SPIONs aggregates are constituted of small nanoparticles, which appeared associated with tiny filaments (Fig. 3F, thin arrow).
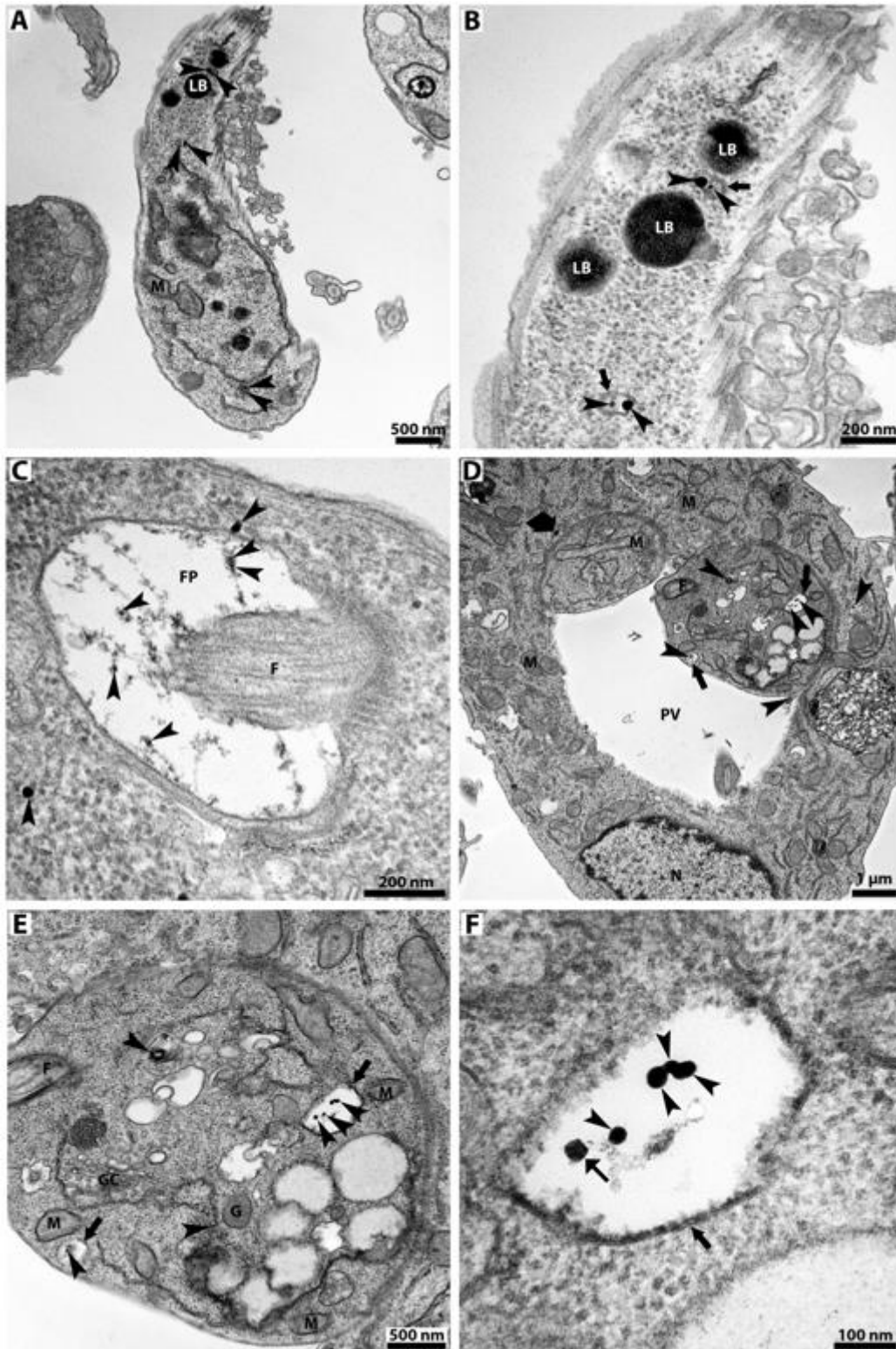
Figures 3A-F. Transmission electron microscopy of *L. amazonensis* promastigotes and intracellular amastigotes treated with 100 µg/mL of SPIONs for 24 h **(A-F)**, where it is possible to observe electrodense aggregates of SPIONs (arrowheads) randomly distributed in both developmental stages. **(A)** SPIONs (arrowheads) were observed in the promastigote cytosol, closely associated with endoplasmic

reticulum profiles and lipid bodies. **(B)** High-magnification image shows that the SPIONs aggregates (arrowheads) can appear inside membrane-bound compartments (arrows). **(C)** SPIONs (arrowheads) are associated with thin filaments inside the flagellar pocket and in the cytosol closely associated with the flagellar pocket membrane. **(D)** In the macrophages infected with intracellular amastigotes, the SPIONs appear inside the parasitophorous vacuole and in the macrophage and parasite cytosol (arrowheads). In this image, it is also possible to observe the SPIONs surrounded by a membrane (arrows) and the presence of an aggregate close to the membrane of the parasitophorous vacuole (large arrow). **(E-F)** Images showing a high magnification of intracellular amastigotes revealed the SPIONs (arrowheads) inside membrane-bound compartments (arrow) and that the aggregates are formed by smaller individual nanoparticles (small arrow). Figure 3E also shows the presence of many lipid bodies, vacuoles, and a multivesicular structure, which are features typically found in treated parasites. F, Flagellum; FP, Flagellar Pocket; LB, Lipid Body; M, Mitochondrion; N, Nucleus; PV, Parasitophorous Vacuole.

Antiproliferative effects of SPIONs in *L. amazonensis* promastigotes and intracellular amastigotes

The analysis of the antiproliferative effects of SPIONs in *L. amazonensis* promastigotes showed that they could not alter the growth for any of the concentrations evaluated (Figure 4A). On the other hand, the SPIONs were very active against intracellular amastigotes (Figure 4B). Furthermore, analysis of the growth curve shows a statistically significant reduction in the percentage of infection for all tested concentrations of SPIONs (1; 5; 10; 25; 50 µg/mL) and treatment times (24, 48, and 72 h) when compared with the control infected macrophages.

After the first 24 h of treatment, it was possible to observe a reduction in the percentage of infection of about 50 % for the concentration of 1 µg/mL and 90 % for 50 µg/mL of SPIONs. The data revealed a concentration-dependent effect, which increased within 48 and 72 h of treatment. The percentage of infection significantly reduces over time, indicating a time-dependent effect. The IC_{50} values were calculated for each

treatment time and confirmed the results obtained (Fig. 4B):   1.206 µg/mL, 0.848 µg/mL, and 0.668 µg/mL for the 24, 48, and 72 h times, respectively.
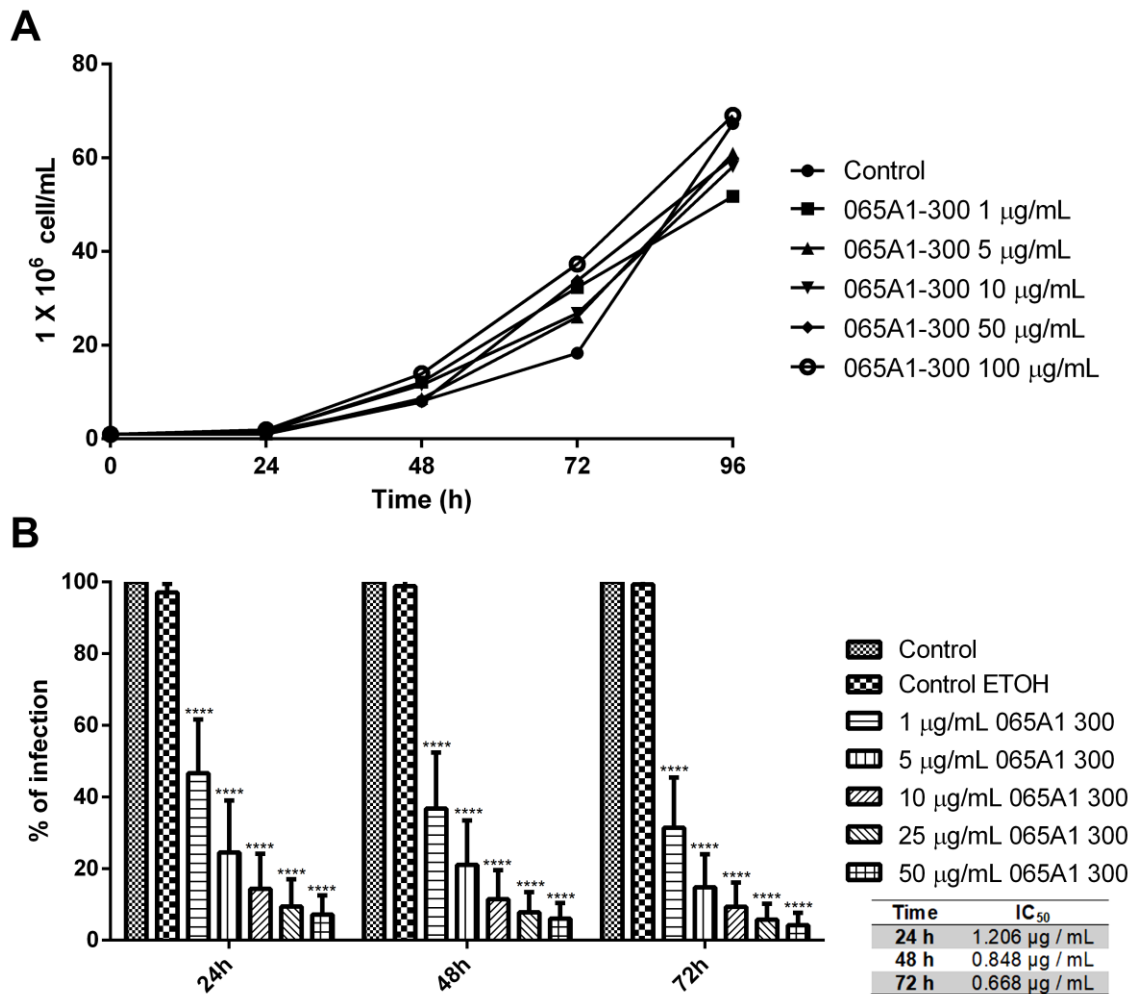
Figures 4A-B. Analysis of the antiproliferative effect in *L. amazonensis* promastigotes and intracellular amastigotes treated with different concentrations of SPIONs. **(A)** Growth curve of *L. amazonensis* promastigotes; the SPIONs were added to the culture medium after 24 h of growth (arrow). **(B)** For intracellular amastigotes, infected macrophages were treated, and the percentage of infection was obtained for each treatment condition; the SPIONs were added to the infected macrophage culture after 24h of infection. *P* values for figure B: **** $p < 0.0001$.

Evaluation of possible effects on the ultrastructure of *L. amazonensis* intracellular amastigotes

Transmission electron microscopy allows us to analyze the possible ultrastructural alterations induced by treating *L. amazonensis* intracellular amastigotes with 100 µg/mL of SPIONs for 24 h (Figs. 5A-D). The images revealed several alterations, such as 1) The presence of lipid bodies (Figure 5A-C, thin arrows); 2) Cytoplasmic disorganization with the presence of many vacuoles, which may indicate activation of autophagic processes (Figure 5A-C, arrows); 3) Presence of myelin-like figures (Figure 5A, arrowhead) and mitochondrial swelling (Figure 5C, star). Furthermore, in some images, it is possible to observe in the intracellular amastigotes the presence of membrane-bound compartments containing SPIONs aggregates and parasitophorous vacuoles containing cellular debris and dead amastigotes (Fig. 5, triangle).
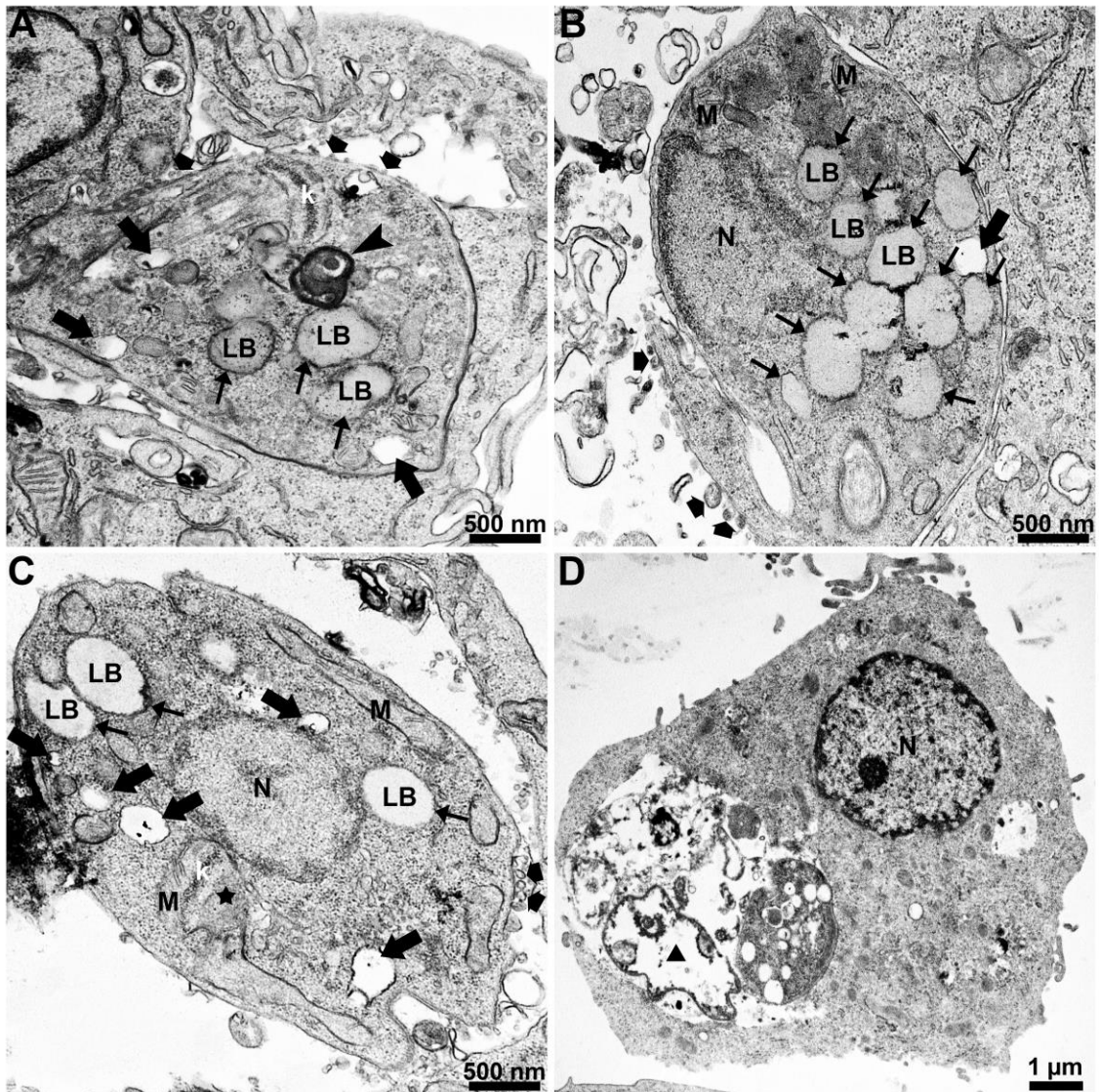
Figures 5A-D. Transmission electron microscopy of *L. amazonensis* intracellular amastigotes treated with 100 µg/mL of SPIONs for 24 h. Different ultrastructural changes were observed in intracellular amastigotes: 1) the presence of many lipid bodies (**A-C**, thin arrows); 2) increased secretion of extracellular vesicles (**A-C**, broad arrow); 3) intracellular vacuolization (**A-C**, arrow); 4) myelin-like figures (**A**, arrowhead); 5) mitochondrial swelling (**C**, star); 6) destroyed amastigotes (**D**, triangle). F, Flagellum; k, kinetoplast; LB, Lipid Body; M, Mitochondrion; N, Nucleus.

Discussion

SPIONs represent a new approach to diagnosing and treating diseases, particularly when associated with magnetic hyperthermia, an emerging form of active treatment [13-17]. However, despite all their potential, the synthesis processes of the SPIONs are characterized by being expensive and toxic to humans and the environment [6]. In this scenario, our group demonstrated the therapeutic potential of low-cost biocompatible SPIONs produced by green synthesis [18]. Thus, the present study aimed to evaluate *in vitro* the therapeutic potential of SPIONs produced with coconut water to treat cutaneous leishmaniasis caused by *Leishmania amazonensis*.

The microscopic techniques efficiently revealed the uptake and distribution of SPIONs in *L. amazonensis* promastigotes and intracellular amastigotes. The first analysis confirmed the uptake of SPIONs by macrophages, which was published previously by our group [18]. Furthermore, in this new article, the images revealed the presence of SPIONs inside the parasitophorous vacuole and in the cytosol of intracellular amastigotes. In addition, SPIONs were also observed randomly distributed throughout the cytosol of promastigotes, in the flagellar pocket, and inside membrane-bound structures. It was the first time that superparamagnetic iron oxide nanoparticles (SPIONs) were observed inside the *Leishmania* spp and the parasitophorous vacuole. The chemical element mapping analysis by scanning electron microscopy confirmed the ferrous nature of the nanoparticle aggregates. These results prove the ability of both promastigote and intracellular amastigote to uptake SPIONs from the culture medium.

The acquisition of iron by *Leishmania* intracellular amastigotes that live inside the mammalian host cells is important for cell differentiation and the pathogenesis of the disease [19-21]. Thus, it is possible to speculate that SPIONs use iron transport mechanisms to reach the parasitophorous vacuole and amastigote cytosol [20].

However, new studies need to be carried out to confirm this hypothesis to elucidate the mechanisms of SPION uptake in promastigotes and amastigotes.

In the sequence, we evaluated the antiproliferative effects of SPIONs in *L. amazonensis* promastigotes and intracellular amastigotes. Despite being internalized by promastigotes, SPIONs did not affect the cell proliferation of the parasites (Fig. 4A). On the other hand, a completely different result was observed for intracellular amastigotes, where the reduction in the percentage of infection was very significant with the lower concentration of SPIONs used [1 µg/mL] (Fig. 4B). The IC_{50} values found for intracellular amastigotes during the treatment were 1.206 µg/mL, 0.848 µg/mL, and 0.668 µg / mL for the times of 24, 48 and 72 h, respectively. In a previous study published by our group, we analyzed the cytotoxicity of SPIONs against the macrophages [18]. The results revealed a non-toxic effect until the concentration of 300 µg/mL, indicating that SPIONs are well-tolerated by the macrophages. These data allow us to estimate the CC_{50} as observed in table 1.

Table 1. Estimate CC_{50} obtained from the analysis of macrophage cytotoxicity assay previously published in Verçoza *et al.* [18].

Time	Estimated cytotoxic concentration of 50 % (CC_{50}) for macrophages
24 h	1,271.5 µg / mL
48 h	2,250.6 µg / mL
72 h	3,420.0 µg / mL

Finally, due to the difficulty of obtaining precise CC_{50} values for the SPIONs, we decided to calculate the selectivity index (SI) using the highest concentration evaluated to treat macrophages and the estimated CC_{50} value to give the highest degree

of reliability in the data (Table 2). The SI revealed that the SPIONs were highly selective for *L. amazonensis* intracellular amastigotes, presenting values significantly higher when compared with other compounds and drugs used to treat *Leishmania* sp. (Table 3) [23-28]. These data indicate a high selectivity index for SPIONs compared with current treatments, different from most compounds, drugs, and nanomaterials developed in the last decades.

Table 2. Selectivity index values were obtained using CC_{50} values of 300 µg/mL and the estimated value from the cytotoxicity assay published in Verçoza *et al.* 2019 [18].

Time	Selectivity Index	
	For CC_{50} = 300 µg/mL	**For estimated CC_{50}**
24 h	248	1,054
48 h	353	2,654
72 h	449	5,119

Table 3. Selectivity index values for different compounds and drugs studied and used for treating leishmaniasis.

Time	Compound	SI	Reference
24 h	Amphotericin B	16	[26]
48 h	TC95	24	[23]
48 h	KH-TFMDI	81	[22]
72 h	Itraconazole	103.17	[25]
72 h	Ravuconazole	28.9	[24]
72 h	Miltefosine	34.2	[27]

During TEM analyses, we observed that intracellular amastigotes were undergoing substantial ultrastructural alterations (Figure 5) when treated with SPIONs, such as 1) accumulation of lipid bodies; 2) intense intracellular vacuolization; 3) mitochondrial swelling; 4) presence of myelin-like figures; and 5) cell death. The observed ultrastructural effects corroborate the significant antiproliferative effect found and give indications of the possible mechanisms of action of these nanoparticles that may be closely associated with intracellular iron homeostasis.

Iron homeostasis has been extensively studied over the years due to its essential role in maintaining the cellular functions of several cell types. In mammalian cells, it is well characterized that the presence of iron in its free state has the potential to participate in the reaction of the Haber-Weiss chemistry acting as a catalyst in the formation of highly reactive hydroxyl radicals that lead the cell to oxidative stress [28-29]. Thus, one of the possibilities for the observed antiproliferative effects could be the result of an imbalance in iron homeostasis with consequent induction of oxidative stress and death of the parasites as followed through TEM. However, further studies need to be carried out to confirm this hypothesis. In *Leishmania,* it is well known that available iron is an important influence on the homeostasis of reactive oxygen species [30]. Studies have already shown that iron overload in the diet of mice causes a decrease in the replication of *Leishmania* spp. in different tissues of infected animals due to the interaction with reactive oxygen and nitrogen species [31-32].

Several studies have shown the potential of using nanoparticles as a new method for treating leishmaniasis. However, few studies still report the effects of using iron oxide nanoparticles [10,11,14,33-35]. Recently, the effects of magnetic iron oxide nanoparticles were demonstrated in *L. mexicana* axenic amastigotes. First, the

amastigotes were treated with 200 µg/mL of magnetic nanoparticles. Then, in sequence, magnetic hyperthermia was applied using an alternating field of 30 mT with a frequency of 452 kHz for 40 min. The results obtained from this study concluded that magnetic hyperthermia was efficient in killing *L. mexicana* axenic amastigotes [10]. Furthermore, another study demonstrated the anti-*Leishmania* effect of magnetic nanoparticles synthesized by green chemistry in *L. major* promastigotes [36]. Finally, a study showed the effect *in vitro* and *in vivo* of amphotericin B encapsulated in magnetic iron oxide nanoparticles coated with glycine-rich peptides for treating visceral leishmaniasis caused by *L. donovani* [11]. All these studies demonstrated the potential gain of drug conjugation with magnetic nanoparticles for treating leishmaniasis.

Conclusion

The use of SPIONs synthesized with coconut water to treat macrophages infected with *Leishmania amazonensis* intracellular amastigotes revealed a significative anti-*Leishmania* effect with a selectivity index higher than 240 times. Furthermore, it was also observed that the SPIONs could be directed into the parasitophorous vacuoles of infected cells and parasites. Thus, this new nanomaterial is a promising new therapeutic alternative for being: 1) an active treatment agent due to its intrinsic properties; 2) a treatment agent associated with heating through an alternate magnetic field; and 3) a drug carrier.

Finally, SPIONs can be considered a strong candidate for a new therapeutic approach to treating cutaneous leishmaniasis, an accessible and low-cost topical treatment.

Experimental

SPIONs

The SPIONs used in the present study were synthesized as described in Verçoza *et al*. 2019 [18] (patent application registration **BR 10 2020 015814** [37]). For assays, after the synthesis and purification, the SPIONs were dispersed in a 70 % ethanol solution (Merck®, Germany). The maximum ethanol concentration in cultures did not exceed 0.5 %, which did not interfere with cell growth. The nanoparticles used in the biological tests were stored at -20°C.

Ethics Committee for the use of laboratory animals

The assays that used mammalian macrophages and parasites from animal models were approved by the Ethics Committee for the Use of Laboratory Animals (CEUA) of the Centro de Ciências da Saúde from the Universidade Federal do Rio de Janeiro according to the Brazilian Federal Law (11794/2008, Decreto No. 6,899/2009). For the use of peritoneal macrophages resident in mice and maintenance of *Leishmania amazonensis* species in Balb/C mice, the protocol number was **UFRJ/CCS-142/21.** Furthermore, according to the guide published by the Brazilian Society of Zootechnics of Laboratory and Council National Control of Animal Experimentation, all animals received human care.

Cell culture

The immortalized murine macrophages RAW 264.7 were grown in 25 cm^2 bottles in RPMI 1640 medium (Cultilab, Brasil) supplemented with 2 % sodium bicarbonate, 10 % fetal bovine serum, and 100 U/mL penicillin. Cells were cultured at 37°C in a 5 % CO_2 atmosphere, and the medium was changed three times a week; cells were passed when they reached the confluence in the bottles. In addition, primary

cultures of murine macrophages were obtained from the peritoneal cavity of CF1 mice by washing with Hanks' balanced solution. Then, they were plated on coverslips in a 24-well culture plate and placed to adhere for 24 h at 37° C with an atmosphere of 5 % CO_2. For the microscopic analyses, macrophages were grown in 25 cm^2 bottles or on glass coverslips in 24-well plates; after 24 h of culture, they were treated for 24 h with different SPION concentrations. This study used WHOM/BR/75/JOSEFA *Leishmania amazonensis* strain as a standard model for cutaneous leishmaniasis. The parasites were maintained according to previously published protocols [22].

Prussian blue staining

For staining with Prussian blue (Sigma-Aldrich, Germany), promastigote and intracellular amastigotes were treated with 100 µg/mL of SPIONs for 24 h. The promastigotes (control and treated cells) were washed in phosphate-buffered saline (PBS) pH 7.2 and adhered for 10 min on glass coverslips previously coated with poly-L-Lysine (Sigma-Aldrich, Germany). The intracellular amastigotes were obtained after infection of RAW 264.7 macrophages at a ratio of 10 parasites to 1 macrophage. After treatment, cells were washed in PBS (pH 7.2), fixed, and dehydrated, as described in Verçoza *et al*. 2019 [18]. Finally, cells were observed in a DM2500 optical microscope (Leica Microsystem, Germany) in bright field mode (BF).

Scanning and transmission electron microscopy analysis

Control and treated cells were washed in PBS pH 7.2, fixed, and post-fixed according to previously published protocols [23]. Then, cells were processed for scanning electron microscopy (SEM) and chemical element mapping analysis, as described in Verçoza *et al*. 2019 [18]. The micrographs were obtained using SEM

TESCAN VEGA 3 LMU operating at 20 kV associated with an OXFORD X-MaxN 20 mm^2 detector (Oxford Instruments, United Kingdom) for the analysis of X-ray energy dispersive spectroscopy (EDS). For transmission electron microscopy (TEM), after fixation, samples were dehydrated in increasing acetone concentrations and embedded in Epon. Ultrathin sections were obtained using a PT-PC PowerTome ultramicrotome (RMC Boeckeler, USA) stained with uranyl acetate and lead citrate and observed using a TEM FEI TECNAI SPIRIT operating at 120 kV.

Antiproliferative effects of SPIONs in *Leishmania amazonensis* promastigotes and intracellular amastigotes

To evaluate the effect of the SPIONs on the growth of *L. amazonensis* promastigotes, cell density experiments were initiated with an inoculum of 1.0×10^6 parasites/mL in M199 culture medium supplemented with 10 % fetal bovine serum and cultivated at 25 °C. After 24 h of growth, different concentrations of SPIONs (1; 5; 10; 50; 100 µg/mL) were added, and cells were cultured for 96 h. The cell density was calculated every 24 h by counting the number of cells in a Neubauer chamber using contrast-phase light microscopy. Besides, SPIONs were also evaluated against intracellular amastigotes, the clinically relevant stage of leishmaniasis; for this analysis, murine macrophages and parasites were obtained as previously published [23]. After 24 h of the initial infection, different concentrations of SPIONs (1; 5; 10; 25; 50 µg/mL) were added, and the medium with the nanoparticles was changed every day for 3 days. The IC$_{50}$ was calculated using the linear regression method defined in a previous study [36].

Statistical analysis

Statistical analysis was conducted using GraphPad Prism with one-way analysis of variance (ANOVA). The results were considered statistically significant for cases $p \leq 0.05$ (*).

References

1. World Health Organization (WHO). Disease factsheet 2019 – Leishmaniasis, 2019.

2. Chakravarty, J.; Sundar, S. *J Glob Infect Dis* **2010**, 2, 167-176.

3. Croft, S. L.; Sundar, S.; Fairlamb, A. H. *Clin Microbiol Rev* **2006**, 19, 111-126.

4. Ponte-Sucre, A.; Padrón-Nieves, M. *Drug Resistance in Leishmania Parasites*. Springer Nature, Switzerland, 2018.

5. Khoo, S. H.; Bond, J.; Denning, D. W. *J Antimicrob Chemother* **1994**, 33, 203-213.

6. Bobo, D.; Robinson, K. J.; Islam, J.; Thurecht, K. J.; Corrie, S. R. *Pharm. Res.* **2016**, 33, 2373-2387.

7. Barick, K. C.; Aslam, M.; Lin, Y. P.; Bahadur, D.; Prasad, P. V., Dravid, V.P. *J. Mater. Chem.* **2009**, 19, 7023-7029.

8. Lee, J. H.; Jang, J-t.; Choi, J-s.; Moon, S.H.; N., S-h.; Kim, J-w.; Kim, J. G.; Kim, I. S.; Park, K. I.; Cheon, J. *Nat. Nanotechnol* **2011**, 6, 418-422.

9. Abazari, R.; Mahjoub, A.R.; Molaie, S.; Ghaffarifar, F.; Ghasemi, E.; Slawin, A. M. Z.; Carpenter-Warren, S. L. *Ultrason. Sonochem* **2018**, 43, 248-261.

10. Berry, S.L.; Walker, K.; Hoskins, C.; Telling, N.D.; Price, H. P. *Sci. Rep.* **2019**, 9, 1-9.

11. Kumar, R.; Pandey, K.; Sahoo, G.C.; Das, S.; Das, V. N. R.; Topno, R. K.; Das, P. *Mater. Sci. Eng C.* **2017**, 1465-1471.

12. Zomorodian, K.; Veisi, H.; Mousavi, S.M.; Ataabadi, M. S.; Yazdanpanah, S.; Bagheri, J.; Mehr, A. P.; Hemmati, S.; Veisi, H. *Int. J. Nanomedicine* **2018**, 13, 3965-3973.

13. Chang, E.H.; Harford, J.B.; Eaton, M.A.W.; Boisseau, P. M.; Dube, A.; Hayeshi, R.; Swai, H.; Lee, D. S. *Biochem. Biophys. Res. Commun.* **2015**, 468, 511-517.

14. Khatami, M.; Alijani, H.; Sharifi, I.; Sharifi, F.; Pourseyedi, S.; Kharazi, S.; Nobre, M. A. L.; Khatami, M. *Sci. Pharm.* **2017**, 85, 36, 1-9.

15. Lee, M.S.; Su, C-M.; Yeh, J-C.; Wu, P-R.; Tsai, T-Y.; Lou, S-L. *Int. J. Nanomedicine* **2016**, 11, 4583-4594.

16. Ranmadugala, D.; Ebrahiminezhad, A.; Manley-Harris, M.; Ghasemi, Y.; Berenjian, A. *Biotechnol. Lett.* **2017**, 40, 237-248.

17. Yang, Y.; Wang, F.; Zheng, K.; Deng, L.; Yang, L.; Zhang, N.; Ran, H.; Wang, Z.; Wang, Z.; Zheng, Y. *et al. PLoS One* **2017**, 12, e0177049.

18. Verçoza, B. R. F.; Bernardo, R. R.; Pentón-Madrigal, A.; Sinnecker, J. P.; Rodrigues, J. C. F.; de Oliveira, L. A. S. *Nanomedicine* **2019**, 14, 2293-2313.

19. Flannery, A. R.; Renberg, R. L.; Andrews, N. W. *Curr. Opin. Microbiol* **2013**, 16, 716-721.

20. Huynh, C.; Andrews, N. W. *Cell. Microbiol* **2008**, 10, 293-300.

21. Mittra, B.; Andrews, N. W. *Trends Parasitol* **2013**, 29, 489-496.

22. Verçoza, B. R. F.; Godinho, J. L. P; Macedo-Silva, S. T.; Huber, K.; Bracher F.; de Souza, W.; Rodrigues, J. C. F. *Apoptosis* **2017**, 22, 1169-1188.

23. Godinho, J. L. P.; Georgikopoulou, K.; Calogeropoulou, T.; de Souza, W.; Rodrigues, J. C. F. *Exp Parasitol* **2013**, 135, 153-165.

24. Macedo-Silva, S. T.; Visbal, G.; Godinho, J. L. P.; Urbina, J. A.; de Souza, W.; Rodrigues, J. C. F. *J. Antimicrob. Chemother* **2018**, 73, 2360-2373.

25. Azevedo-França, J. A.; Granado, R.; Macedo-Silva, S. T.; Santos-Silva, G.; Scapin, S.; Borba-Santos, L. P.; Rozental, S.; de Souza, W.; Martins-Duarte, E. S.; Barrias, B.; Rodrigues, J. C. F.; Navarro, M. *Antimicrob. Agents Chemother*

2020, 64, 1-15.

26. Caldeira, L.R.; Fernandes, F. R.; Costa, D. F.; Frézard, F.; Afonso, L. C.; Ferreira, L. A. *Eur. J. Pharm. Sci.* **2015**, 70, 125-131.

27. Stroppa, P. H. F.; Antinarelli, L. M. R.; Carmo, A. M. L.; Gameiro, J.; Coimbra, E. S.; da Silva, A. D. *Bioorg. Med. Chem* **2017**, 25, 3036-3045.

28. Emerit, J.; Beaumont, C.; Trivin, F. *Biomed. Pharmacother* **2001**, 55, 333-339.

29. Mccord, J. M. *Blood,* **2004**, 11, 3171-3172.

30. Taylor, M. C.; Kelly, J. M. *Parasitology* **2010**, 137, 899-917.

31. Vale-Costa, S.; Gomes-Pereira, S.; Teixeira, C. M; Rosa, G.; Rodrigues, P. N.; Tomás, A.; Appelberg, R.; Gomes, M. S. *PLoS Negl. Trop. Dis.* **2013**, 7, e2061.

32. Bisti, S.; Konidou, G.; Papageorgiou, F.; Milon, G.; Boelaert, J. R.; Soteriadou, K. *Eur. J. Immunol* **2000**, 30, 3732-3740.

33. Nafari, A.; Cheraghipour, K.; Sepahvand, M.; Shahrokhi, G.; Gabal, E.; Mahmoudvand, H. *Parasite Epidemiol. Control* **2020**, 10, e00156.

34. Akbari, M.; Oryan, A.; Hatam, G. *Acta Trop.* **2017**, 172, 86-90.

35. Della Pepa, M.E.; Martora, F.; Finamore, E.; Vitiello, M.; Galdiero, M.; Franci G. In *Nanotechnology Applied to Pharmaceutical Technology*; Rai, M.; dos Santos, C. A. Eds.; Springer Nature, Switzerland, 2017; pp. 307-333.

36. Martin, M. B.; Grimley, J. S; Lewis, J. C.; Heath, H. T.; Bailey, B. N.; Kendrick, H.; Yardley, V.; Caldera, A.; Lira, R.; Urbina, J. A.; Moreno, S. N. J.; Docampo, R.; Croft, S. L.; Oldfield, E. *J. Med. Chem.* **2001**, 44, 909-916.

37. Verçoza, B. R. F.; Bernardo, R. R.; Pentón-Madrigal, A.; Sinnecker, J. P.; Rodrigues, J. C. F.; de Oliveira, L. A. S. Method for the sustainable production of superparamagnetic iron oxide nanoparticles. B.R. Pat. Appl. BR 10 2020 015814 7, Aug 3, 2020.